Article

Artificial Neural Network Modeling Techniques for Drying Kinetics of *Citrus medica* Fruit during the Freeze-Drying Process

Muhammed Emin Topal [1,*] **, Birol Şahin** [1] **and Serkan Vela** [2]

1 Faculty of Engineering and Architecture, Department of Mechanical Engineering,
Recep Tayyip Erdogan University, 53100 Rize, Türkiye; birol.sahin@erdogan.edu.tr
2 Electronics and Communication Engineering, Of Technology of Faculty, Karadeniz Technical University,
61830 Trabzon, Türkiye; serkanvela@ktu.edu.tr
* Correspondence: muhammedemin.topal@erdogan.edu.tr

Abstract: The main objective of this study is to analyze the drying kinetics of *Citrus medica* by using the freeze-drying method at various thicknesses (3, 5, and 7 mm) and cabin pressures (0.008, 0.010, and 0.012 mbar). Additionally, the study aims to evaluate the efficacy of an artificial neural network (ANN) in estimating crucial parameters like dimensionless mass loss ratio (MR), moisture content, and drying rate. Feedforward multilayer perceptron (MLP) neural network architecture was employed to model the freeze-drying process of *Citrus medica*. The ANN architecture was trained using a dataset covering various drying conditions and product characteristics. The training process, including hyperparameter optimization, is detailed and the performance of the ANN is evaluated using robust metrics such as RMSE and R^2. As a result of comparing the experimental MR with the predicted MR of the ANN modeling created by considering various product thicknesses and cabin pressures, the R^2 was found to be 0.998 and the RMSE was 0.010574. Additionally, color change, water activity, and effective moisture diffusivity were examined in this study. As a result of the experiments, the color change in freeze-dried *Citrus medica* fruits was between 6.9 ± 0.2 and 21.0 ± 0.6, water activity was between 0.4086 ± 0.0104 and 0.5925 ± 0.0064, effective moisture diffusivity was between 4.19×10^{-11} and 21.4×10^{-11}, respectively. In freeze-drying experiments conducted at various cabin pressures, it was observed that increasing the slice thickness of *Citrus medica* fruit resulted in longer drying times, higher water activity, greater color changes, and increased effective moisture diffusivity. By applying the experimental data to mathematical models and an ANN, the optimal process conditions were determined. The results of this study indicate that ANNs can potentially be applied to characterize the freeze-drying process of *Citrus medica*.

Keywords: artificial neural network; freeze-drying; mathematical modeling; drying kinetics; *Citrus medica*

1. Introduction

Citrus medica fruit is a tropical plant species that is very resistant to cold weather, and has a pleasant smell and larger fruits than other citrus species. Citron fruits are quite large, yellow, and have a thick, bumpy peel with many seeds [1]. It is known that *Citrus medica* fruit has numerous benefits such as anticold, capillary protector, antihypertensive, diuretic, antibacterial, analgesic, strong antioxidant, antidiabetic, and antihyperglycemic, which have been proven by pharmacological studies [2,3]. *Citrus medica* fruit, a plant rich in vitamin C, is one of the three true citrus varieties, and fruits such as orange, lemon, and sour orange are obtained through hybridization of these varieties [4]. Many different products such as marmalade, jam, candies, tea, and carbonated drinks can be obtained from *Citrus medica* fruit. The moisture content of *Citrus medica* fruit is approximately 78% [2].

Drying is a fundamental operation in food processing, aimed at reducing moisture content to improve shelf life, prevent spoilage, and maintain product quality [5]. Drying can be accomplished through various methods such as solar-assisted drying, hot-air drying,

fluidized-bed drying, shade drying, and freeze-drying [6]. Compared to traditional drying methods, freeze-drying minimizes losses in properties such as color, flavor, and aroma, and provides higher rehydration rates and longer storage times [7]. Freeze-drying is a process that removes ice crystals from a frozen product under low pressure through sublimation [8]. Upon reviewing the literature, it is found that many products, including strawberry [9], persimmon [10], tomatoes [11], chokeberry [12], okra [13], and red pepper [14], have been dried through the freeze-drying method and thin-layer drying kinetics have also been evaluated.

Accurate prediction of drying parameters has a crucial role in optimizing process conditions, minimizing energy consumption, and ensuring consistent product quality. Artificial neural networks (ANNs) have become invaluable tools for modeling complex relationships across various domains, including food processing. A model that can accurately predict the drying operation depending on input variables such as product thickness, cabin pressure, and drying time by harnessing the predictive power of ANNs is critical in terms of time-saving and energy consumption. Various products and drying methods, such as apple [15], potato [16], mushroom [17], thyme leaves [18], Mentha spicata l. [19], and white mulberry [20] have been subjected to ANN analysis according to studies in the literature. Selvi et al. (2022) [21] conducted infrared drying of linden leaves and applied artificial neural networks (ANN) to the data obtained during the experiment to determine the drying kinetics. They observed that the mass change in the linden leaf during the drying process, when applied to commonly used thin-layer drying models in the literature, such as the Page, Midilli et al., Henderson and Pabis, logarithmic, and Newton models, resulted in R^2 values > 0.9900 and RMSE values < 0.0025. The ANN model, on the other hand, showed R^2 and RMSE values of 0.9986 and 0.0210, respectively. Additionally, they observed a high degree of agreement between the predicted values generated by the ANN model and the experimental moisture content data. In their study, Zalpouri et al. (2023) [22] conducted drying experiments on onion puree of varying thicknesses using refractance-window drying and convective drying methods. They applied the experimental data to eight different thin-layer drying models and used a multilayer feedforward ANN to predict the dimensionless mass loss ratio (MR) of the onion puree. Their results indicated that both the Lewis model and the Wangh and Singh model were the most accurate in describing the drying process, and that the ANN was competitive with these models. Khaled et al. (2020) [23] conducted drying experiments on persimmon fruit slices of varying thicknesses using vacuum drying and hot-air drying methods. To describe the drying kinetics, they employed multilayer feedforward artificial neural networks (ANNs), support vector machines (SVM), and k-nearest neighbors (kNN) methods. The R^2 values obtained using the ANN, SVM, and kNN methods were 0.9994, 1.0000, and 0.9327, respectively. The study concluded that computational intelligence methods can be reliably used to describe the drying kinetics of persimmon fruits.

As in all sectors, time, energy consumption, and cost-effectiveness are of utmost importance in the food drying and processing industry. Additionally, it is essential to preserve specific characteristics of the food such as color, taste, and shape to appeal to consumers. In this study, freeze-drying, which minimizes quality losses in the product when considering drying methods, was chosen for the drying of *Citrus medica* fruit. The data obtained during the freeze-drying process were applied to various mathematical models found in the literature and to the ANN. Furthermore, comparisons were made between the ANN, which has superior learning capacity and better flexibility, with an online, nonintervention structure method along with traditional mathematical modeling methods. While mathematical modeling only predicts MR changes, an ANN predicts changes in MR, MC, and DR. By employing an ANN to elucidate the drying process of *Citrus medica* fruit and optimize the corresponding process conditions, it is possible to achieve significant reductions in time, energy consumption, and costs. Despite all the drying studies carried out on the products, no study has been found on drying the *Citrus medica* fruit by the freeze-drying method and investigating the thin-layer drying

kinetics together with applying an ANN during the drying process. Drying kinetics of *Citrus medica* dried with the freeze-drying method were examined experimentally and the obtained data were applied to six thin-layer mathematical models (Aghbaslo, Alibas, Balbay and Sahin, improved Midilli–Kucuk, Newton, and Page) preferred in the literature. Thin-layer mathematical models and an ANN structure are used to define the drying kinetics of the *Citrus medica* fruit. The objective of this research is to investigate how freeze-drying with varying cabin pressures (0.008, 0.010, and 0.012 mbar) affects the drying behavior of *Citrus medica* fruit slices with various thicknesses (3, 5, and 7 mm). The study also aims to develop an ANN-based model to predict the drying kinetics of the dried *Citrus medica* fruit. Thus, it is aimed to use the ANN to establish a meaningful connection among features such as cabin pressure, product thickness, drying time, and drying kinetics.

2. Materials and Methods

2.1. Material

The samples of *Citrus medica* used for the drying experiment were harvested in Rize Province, Türkiye (41.030290° N, 40.489494° E), in December 2023. The bumpy peel was removed from the samples prior to freeze-drying, and *Citrus medica* fruits were sliced into thicknesses of 3, 5, and 7 mm before being frozen at $-40\,°C$ for 24 h. To determine the initial moisture content of *Citrus medica*, a 50 g sample was placed in an oven (Jeio Tech-ON-21E, Jeio Tech Co., Daejeon, Republic of Korea) operating at a constant temperature (105 °C) for 24 h. The moisture content was determined to be $81.0 \pm 0.1\%$.

2.2. Methods

2.2.1. Drying Procedure

The frozen *Citrus medica* fruits were placed in a Labconco FreeZone 2.5 Manual freeze dryer (Labconco, Kansas City, MO, USA) and subjected to various pressure values (0.008, 0.010, and 0.012 mbar) for drying. The mass of the product was measured and recorded during the experiments using a precise balance (DIKOMSAN EGY-50, with a sensitivity of 10^{-3} g, Dikomsan, Istanbul, Türkiye) located inside the drying chamber.

2.2.2. Determination of Moisture Content, Dimensionless Mass Loss Ratio, and Drying Rate

Drying is defined as the process of prolonging the storage duration of a product by reducing its moisture content (MC) to a level where microbial growth will not occur. In this regard, it is very important to determine the initial moisture content of the product to be dried and the moisture content of the final product. The moisture content of *Citrus medica* fruit was calculated using Equation (1). The most important parameter in the mathematical modeling phase used to describe the drying process is the dimensionless mass loss ratio (MR) determined using Equation (2). In addition, the drying rate (DR) of the product, which varies depending on the moisture content of the product, its thickness, and process conditions (such as temperature and pressure), was determined using Equation (3).

$$MC = \frac{M_0 - M_e}{M_0} \times 100 \tag{1}$$

$$MR = \frac{M_t - M_e}{M_0 - M_e} \tag{2}$$

$$DR = \frac{M_{t+dt} - M_t}{dt} \tag{3}$$

In this equation, M_0, M_e, M_{t+dt}, and M_t are the moisture content at the initial condition, the moisture content at the equilibrium state, the moisture content at times $t + dt$, and the moisture content t, respectively.

2.2.3. Mathematical Modeling of the Drying Data and Statistical Analysis

During the freeze-drying experiments, the mass of the product was measured at specific time intervals using a precise balance located inside the drying chamber, and the MR was calculated. These data were then used to apply thin-film models, as given in Equations (4)–(9). Six thin-film drying models commonly used in the literature are given in Table 1.

Table 1. Thin-layer drying models [21,24–26].

Model Name	Model No.	Model Equation	Equations
Aghbaslo	1	$MR = \exp\left(-\frac{k_1 t}{1 + k_2 t}\right)$	(4)
Alibas	2	$MR = a\exp((-kt^n) + (bt)) + g$	(5)
Balbay and Sahin	3	$MR = (1 - a)\exp(-kt^n) + b$	(6)
Improved Midilli Kucuk	4	$MR = a\exp(-k_1 t^n) - \exp(-k_2 t^n) - bt^n$	(7)
Newton	5	$MR = \exp(-kt)$	(8)
Page	6	$MR = \exp(-kt^n)$	(9)

MR: dimensionless mass loss ratio; k, k_1, k_2, a, b, g: drying constants; n: number of drying constants; t: time.

A nonlinear regression analysis was conducted to examine all experimental data and determine the most suitable model for describing the drying processes. Table 2 presents the evaluation criteria (Equations (10)–(12)) used to assess how well the mathematical models align with the real experimental system. The best model to describe the drying of *Citrus medica* fruit was identified based on the evaluation criteria. The R^2 should have the highest value, while the χ^2 and RMSE should have the lowest value when evaluating the data obtained from the drying experiments [27,28].

Table 2. Criterion equations used in evaluating the mathematical modeling of the drying curve [29].

Evaluation Parameters	Evaluation Criterion Equations	Equations
Reduced chi-square	$\chi^2 = \frac{\sum_{i=1}^{N}\left(MR_{exp,i} - MR_{pre,i}\right)^2}{N - n}$	(10)
Root mean square error	$RMSE = \sqrt{\frac{\sum_{i=1}^{N}\left(MR_{pre,i} - MR_{exp,i}\right)^2}{N}}$	(11)
Coefficient of determination	$R^2 = 1 - \frac{\sum_{i=1}^{N}\left(MR_{exp,i} - MR_{pre,i}\right)^2}{\sum_{1}^{n}\left(MR_{exp,i} - MR_{avg}\right)^2}$	(12)

N: number of observations; exp: experimental; pre: predicted; avg: average.

2.2.4. Artificial Neural Network Design

In this study, feedforward multilayer perceptron (MLP) neural network architecture was employed to model the freeze-drying process of *Citrus medica*. MLPs are widely used for regression tasks and have been successful in modeling drying processes, making them a suitable choice for this study [30–34]. The MLP was implemented using the feedforward-net function in MATLAB R2023a. The architecture comprises an input layer, one hidden layer, and an output layer. The input layer incorporates features relevant to the drying process, including product thickness (I_1), cabin pressure (I_2), and drying time (I_3). These features were selected based on their significant impact on drying kinetics observed in the experimental study. In this study, a single hidden layer with 5 neurons was used. While determining the optimal number of hidden neurons often involves empirical testing, a single hidden layer with a moderate number of neurons has been shown to be sufficient for approximating complex functions in many applications, including drying [33]. For this study, initial experiments indicated that a single hidden layer achieved satisfactory performance. The hidden layer utilized the default activation function in feedforwardnet, which is the tan–sigmoid activation function. The tan–sigmoid function introduces nonlinearity into the model, enabling it to capture the complex relationships between the input features and the output drying parameters. A linear activation function was used for the output

layer. This is a standard practice for regression problems because linear activation allows the network to output a continuous range of values, which is appropriate for predicting drying parameters like moisture content and drying rate. The output layer consists of predicted drying parameters, namely dimensionless mass loss ratio (MR), moisture content (MC), and drying rate (DR). The overall structure of the ANN, including the connections between input, hidden, and output layers, is depicted in Figure 1.
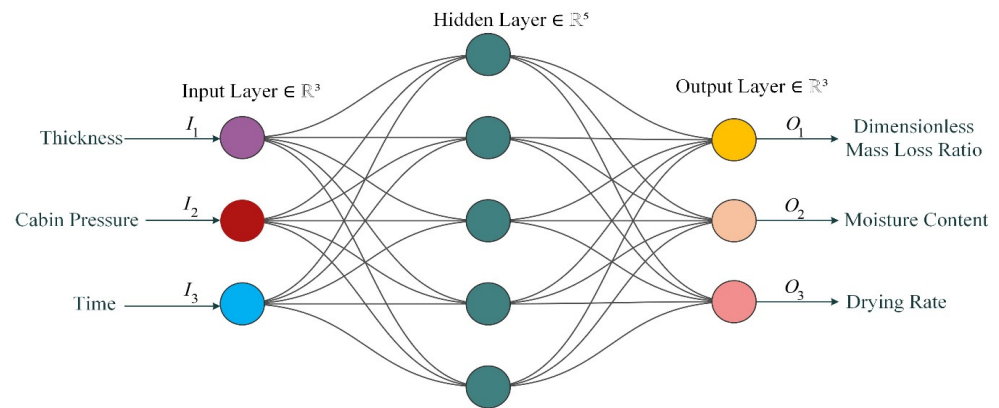
Figure 1. ANN structure applied to learn the freeze-drying process of *Citrus medica* fruit.

The mathematical expressions governing the network's behavior are given in Equations (13)–(15).

Hidden layer activation (a_1):

$$a_1 = f(W_1 \cdot I + b_1) \tag{13}$$

Output layer activation (a_2):

$$a_2 = f(W_2 \cdot a_1 + b_2) \tag{14}$$

Loss function (L):

$$L = \frac{1}{N} \sum \left(\|Y_{true} - Y_{pre}\|^2 \right) \tag{15}$$

where W_1 and W_2 are the weight matrices of the hidden and output layers, respectively; b_1 and b_2 are the bias vectors of the hidden and output layers, respectively; $f(.)$ denotes the activation function (e.g., sigmoid, ReLU); Y_{true} is the true output vector; Y_{pre} is the predicted output vector; and N is the number of samples in the dataset.

The network's weights and biases were optimized using the Levenberg–Marquardt backpropagation algorithm, the default training algorithm for feedforwardnet in MATLAB r2023a. This algorithm is known for its efficiency in finding local minima of the error function, particularly for networks with a moderate number of weights and biases [34], as is the case in this study. The training was performed for a maximum of 1000 epochs. The max_fail parameter, set to 20, implements an early stopping criterion based on the validation set performance to prevent overfitting. If the validation error does not decrease for 20 consecutive epochs, the training process is stopped to avoid overfitting the training data and to improve the model's ability to generalize to unseen data. Other parameters are summarized in Table 3.

Artificial neural networks (ANNs) have been chosen for predicting drying kinetics due to their proven ability to model complex nonlinear relationships. This has been demonstrated in various studies. For instance, Cetin (2022) [35] used ANNs to predict the MR and drying rate of orange slices, while Dalvi-Isfahan (2020) [36] compared different modeling approaches for predicting the moisture content of apple slices. Additionally, Chasiotis et al. (2020) [37] utilized ANNs to model the moisture content evolution during the convective drying of cylindrical quince slices.

Table 3. Algorithm parameters for the training neural network.

Parameter	Value
Number of epochs	1000
Maximum validation failures	20
Minimum gradient	1×10^{-5}
μ parameter	0.01
μ decrease parameter	0.1
μ increase parameter	10

The flexibility and adaptability of ANNs allow them to be customized to match the specific characteristics of a dataset, such as the number of input features and desired outputs. This capability makes them particularly suitable for diverse and complex applications, where models like support vector machines (SVMs) or random forests might be less effective. This is supported by the literature, which shows that ANNs can be finely tuned to the nuances of specific datasets and tasks [38,39].

In the realm of drying processes, ANNs have shown exceptional success. For example, an ANN model effectively predicted the drying kinetics and chemical attributes of linden leaves during infrared drying, achieving high accuracy and demonstrating robustness in handling such tasks. Another study on sweet potato drying processes highlighted the optimization potential of ANNs to enhance various drying methods, emphasizing their adaptability and precision in modeling intricate data relationships [21,40].

The initial exploration using the chosen ANN architecture in this study yielded promising results in predicting drying parameters, providing strong justification for further refinement and evaluation of this model. Although other machine learning models might offer additional insights, the proven track record and customization capabilities of ANNs make them an excellent choice for this specific application [21,40].

Furthermore, the Levenberg–Marquardt backpropagation algorithm, commonly used for training feedforward networks in MATLAB r2023a, enhances the efficiency of ANNs by optimizing weights and biases. This algorithm is particularly suitable for networks with a moderate number of parameters, providing rapid convergence and effective minimization of the error function [41,42], which are crucial for achieving accurate and reliable predictions in drying process models.

In summary, the focus on ANNs in this study is justified by their established effectiveness, flexibility, and the promising initial results obtained with the chosen architecture. This targeted approach allows for more in-depth refinement and evaluation, ultimately aiming to optimize and accurately predict drying parameters [21,30–33,38,40].

2.2.5. Determination of Water Activity

The change in water activity was measured before and after the drying experiments using a water activity meter (Aqualab-Dew Point-Water Activity Meter 4TE). The temperature-controlled sample chamber was set to 25 °C.

2.2.6. Determination of Color Change

The color of the *Citrus medica* fruits was measured at the beginning and end of freeze-drying experiments using a colorimeter (Color Reader CR-10). To determine the color change in the product, the L*, a*, and b* values were measured at three different points on the *Citrus medica* fruit. The colorimeter's L*, a*, and b* values indicate the lightness, redness/greenness, and yellowness/blueness, respectively. The color change in the product as a result of the freeze-drying experiments is calculated using Equation (16).

$$\Delta E = \sqrt[2]{\left(\Delta L^*\right)^2 + \left(\Delta a^*\right)^2 + \left(\Delta b^*\right)^2} \tag{16}$$

where ΔL^* is the lightness difference, Δa^* the redness/greenness difference, and Δb^* the yellowness/blueness difference.

2.2.7. Effective Moisture Diffusivity (D_{eff})

The effective moisture diffusivity describes the rate of moisture movement, regardless of the mechanism involved [43]. The drying of food products mostly occurs in the falling rate period [44]. The calculation of MR can be adopted from a moisture diffusion model based on Fick's Second Law, as shown in Equation (17).

$$MR = \frac{8}{\pi^2} \sum_{m=1}^{\infty} \frac{1}{(2n+1)^2} exp\left(\frac{(2n+1)^2 \pi^2 D_{eff} t}{4L^2}\right) \tag{17}$$

where D_{eff} is the effective moisture diffusivity, and L is the half thickness of the product [45]. Transforming Equation (14) into a linear function of time yields Equation (18).

$$ln(MR) = \ln\left(\frac{8}{\pi^2}\right) + \left(-\frac{\pi^2 D_{eff} t}{4L^2}\right) \tag{18}$$

The slope (k) of t versus ln(MR) can be expressed as a function of D_{eff}, as in Equation (19).

$$k = -\frac{\pi^2 D_{eff}}{4L^2} \tag{19}$$

2.2.8. Uncertainty Analysis

During experimental studies, an uncertainty analysis is performed using Equation (20) to determine the accuracy of the experiment, taking into account many factors such as the sensitivity of the measurement instruments and the environmental conditions under which the experiment is performed [46]. The sensitivity values of the devices used in the experiments are given in Table 4.

$$W_R = \left[\left(\frac{\partial R}{\partial x_1} w_1\right)^2 + \left(\frac{\partial R}{\partial x_2} w_2\right)^2 + \left(\frac{\partial R}{\partial x_3} w_3\right)^2 + \ldots + \left(\frac{\partial R}{\partial x_n} w_n\right)^n\right]^{\frac{1}{2}} \tag{20}$$

where W_R is uncertainty in the results; R is the result as a function of independent variables of x_1, x_2, x_3, and x_n; and w_1, w_2, w_3, and w_n are uncertainties of independent variables.

**Table 4.** Sensitivity of equipment used in the experiments.

Equipment	Uncertainty	Sensitivity
Freezer temperature	w_1	$\pm 1\,^\circ C$
Precision balance	w_2	$\pm 10^{-3}$ g
Freeze-dryer temperature	w_3	$\pm 0.1\,^\circ C$
Freeze-dryer pressure	w_4	± 0.001 mbar
Drying oven temperature	w_5	$\pm 1\,^\circ C$
Digital thermometer	w_6	$\pm 0.1\,^\circ C$
Color meter	w_7	± 0.1
Water activity meter	w_8	± 0.01
Caliper precision	w_9	± 0.01 mm

As a result of the calculations performed and depending on the sensitivity of the measuring devices used in the experimental studies, $W_{R_{FD}} = 1.43\%$ was obtained.

3. Results and Discussions

### 3.1. Effect of the Freeze-Drying Process on Moisture Content and Drying Rate

In this study, the drying process of *Citrus medica* fruit was examined depending on MC, MR, and DR. The changes in calculated MC and DR values depending on drying time are given in this section. The changes in the moisture content of *Citrus medica* fruit over time following the application of the freeze-drying method at various product thicknesses and cabin pressures are illustrated in Figure 2. Through freeze-drying experiments conducted at varying product thicknesses and cabin pressures, it was observed that the 3 mm thick *Citrus medica* fruit dried at 0.008 mbar cabin pressure had the shortest drying time, whereas the 7 mm thick product dried at 0.012 mbar cabin pressure had the longest drying time. The final products obtained from the freeze-drying experiments were compared based on their moisture contents, and it was found that the minimum moisture content was 15.4% for the 3 mm thick product dried at 0.008 mbar, while the highest moisture content was 20% for the 7 mm thick product dried at 0.012 mbar. As the cabin pressure and product thickness increased, the drying time and moisture content of the final product also increased. As seen in Figure 2, reducing the cabin pressure from 0.012 to 0.008 mbar reduces the drying time of the final product. As the cabin pressure decreases, drying the product in a shorter time is consistent with other studies in the literature [47,48]. Additionally, it is expected that the drying time will shorten as the pressure drops further below the triple point (0.01 °C, 6.1173 mbar) of water. In this study, a significant reduction in drying time was observed as the pressure decreased from 0.012 to 0.008 mbar. Furthermore, it was concluded that the product dries for a longer period as the product thickness increases. Similar findings have been reported in the literature, where drying experiments conducted using freeze-drying and many other drying techniques have shown that drying time increases with sample thickness [49–53].
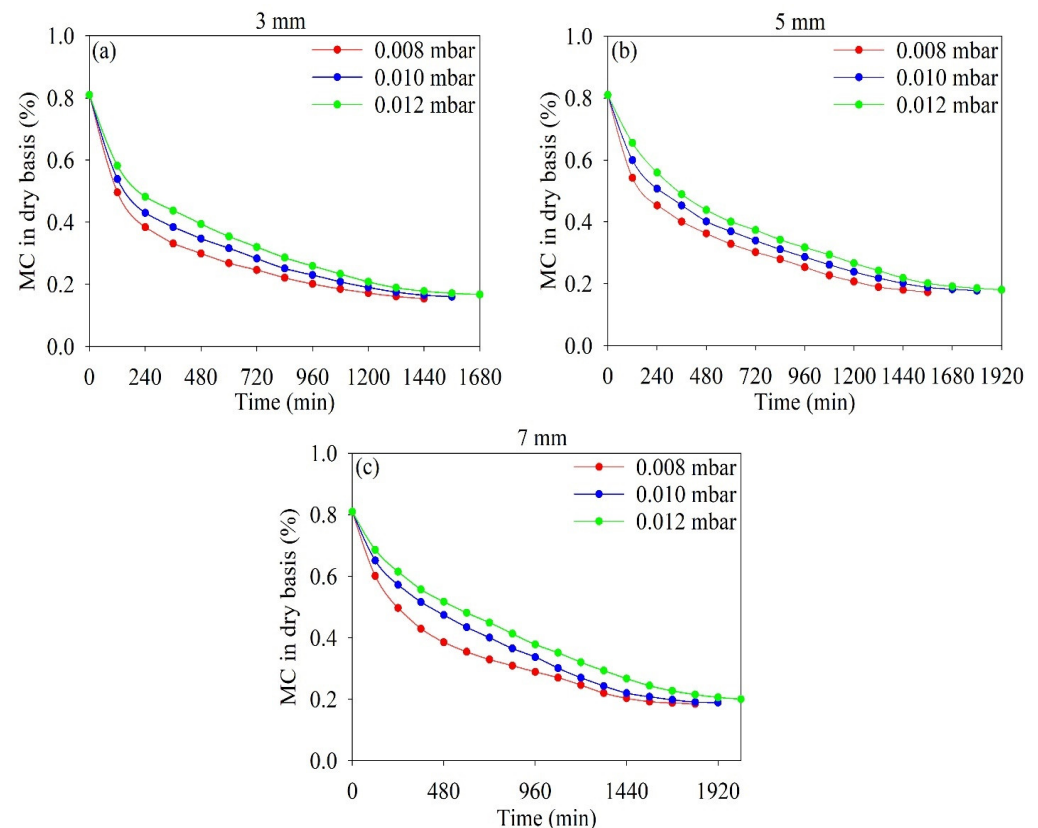
Figure 2. Variation in moisture content of *Citrus medica* fruit depending on thickness and cabin pressure: (**a**) 3 mm, (**b**) 5 mm, and (**c**) 7 mm.

As a result of the experiments carried out at various product thicknesses and cabin pressures, it was observed that the drying process generally took place in the falling speed period, as seen in Figure 3. As the moisture content of the products decreased, the drying speed decreased, and the curves became steeper as the cabin pressure decreased. During freeze-drying of *Citrus medica* fruit, the highest drying rate was calculated to be 0.261%/min (3 mm and 0.008 mbar) when examining Figure 3. It was observed that the drying rate decreased as the pressure in the drying cabin and the thickness of the product increased. Furthermore, it is evident that the drying rate is highest at the beginning and decreases as the moisture content of the product decreases during the drying process. During the freeze-drying experiments, it was observed that the drying rate of *Citrus medica* fruit was in the falling rate period, consistent with existing studies [54–57]. Additionally, it was found that higher drying rates were achieved at lower drying chamber pressures. Various studies in the literature also corroborate this study, showing that the drying rate is initially at its highest value and subsequently decreases as the moisture content of the product diminishes [58–60].
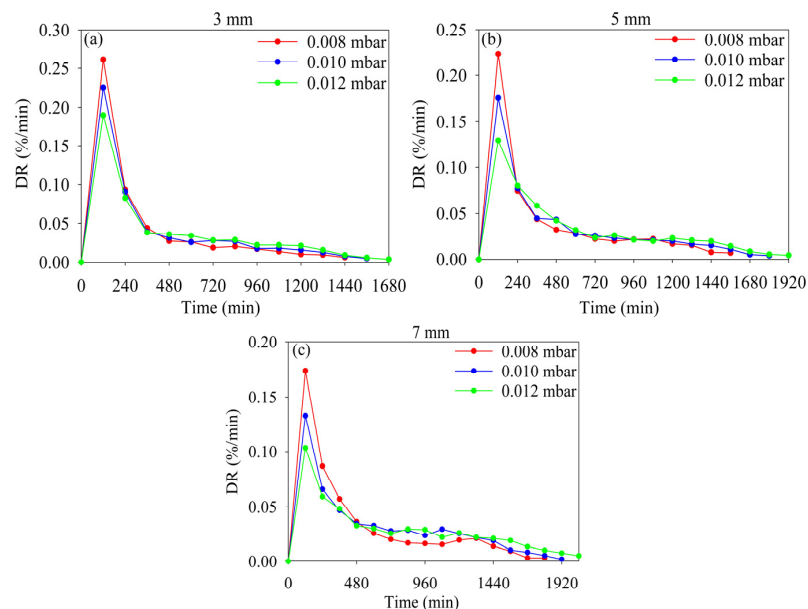
Figure 3. Change in drying rate of *Citrus medica* fruit depending on thicknesses and cabin pressures: (**a**) 3 mm, (**b**) 5 mm, and (**c**) 7 mm.

3.2. Mathematical Modeling and Statistical Analysis Results of the Freeze-Drying Process

After the experimental studies, six models used in the literature for thin-layer freeze-drying of *Citrus medica* fruit and the evaluation criteria used were investigated. When the data obtained from the freeze-drying experiments were evaluated, the R^2 value was the highest (close to 1), while the χ^2 and RMSE values were the lowest (a value close to 0 is targeted). While the R^2 varies between 0 and 1, the mathematical model that yields results closest to 1 is the most suitable model for explaining the behavior and conditions of thin-layer freeze-drying of *Citrus medica* fruit.

Figure 4 shows the MR–drying time curves, which change depending on the freeze-dryer cabin pressure. Upon examination of Figure 4, it was found that lower cabin pressure resulted in shorter freeze-drying time for the product. The results of the evaluation criteria used to determine the mathematical model that best describes the freeze-drying processes at various thicknesses and cabin pressures are shown in Table 5. Considering the mathematical modeling drying-curve evaluation criterion equations, it was seen that the models that best describe the drying process of *Citrus medica* fruit for 3 mm sample thickness are the Alibas (0.008 and 0.010 mbar) and improved Midilli–Kucuk (0.012 mbar) models. It was determined that the improved Midilli–Kucuk (0.008 and 0.012 mbar) and Balbay and

Sahin (0.010 mbar) models are the most suitable models to explain the drying process of *Citrus medica* fruit with 5 mm sample thickness. Considering the evaluation criteria results, it was seen that the models that best describe the freeze-drying process of the 7 mm sample thickness product are the improved Midilli–Kucuk (0.008 mbar) and Balbay and Şahin (0.010 and 0.012 mbar) models. Similar to this study, Midilli and Kucuk [24] stated that the Aghbaslo, Alibas, improved Midilli–Kucuk, and Balbay and Sahin models best predicted the drying kinetics of green tea leaves, apricot, kiwi, and mammoth pumpkin. Dundar et al. [61] found similar results, indicating the evaluation of the suitability of the Newton, Page, Aghbaslo, and Alibas models in a discussion on the hot-air drying and freeze-drying characteristics of Prunus domestica flowers.
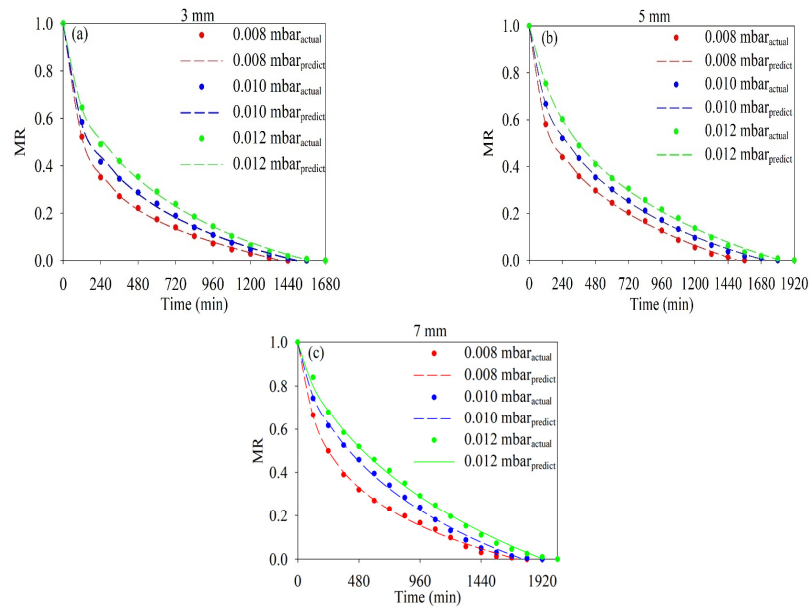
Figure 4. MR variations in drying time depending on thicknesses and cabin pressures: (**a**) 3 mm, (**b**) 5 mm, and (**c**) 7 mm.

Table 5. Evaluation criteria for drying *Citrus medica* fruits with various thicknesses and cabin pressures.

	M	0.008 mbar			0.010 mbar			0.012 mbar		
		R^2	χ^2	RMSE	R^2	χ^2	RMSE	R^2	χ^2	RMSE
3 mm	1	0.99168	0.00102	0.02942	0.98766	0.00164	0.03749	0.98754	0.00181	0.03965
	2	0.99966	0.00006	0.00596	0.99927	0.00013	0.00914	0.99235	0.00145	0.03106
	3	0.99945	0.00008	0.00757	0.99927	0.00012	0.00914	0.99906	0.00016	0.01086
	4	0.99964	0.00006	0.00615	0.99934	0.00012	0.00866	0.99924	0.00014	0.00981
	5	0.97264	0.00308	0.05334	0.97633	0.00290	0.05192	0.98459	0.00208	0.04409
	6	0.99678	0.00040	0.01830	0.98803	0.00159	0.03692	0.99193	0.00117	0.03190
5 mm	1	0.98615	0.00189	0.04030	0.98979	0.00147	0.03589	0.99355	0.00104	0.03031
	2	0.99967	0.00006	0.00620	0.97312	0.00493	0.05823	0.99931	0.00014	0.00995
	3	0.99967	0.00005	0.00623	0.99961	0.00007	0.00700	0.99929	0.00013	0.01009
	4	0.99969	0.00006	0.00599	0.99950	0.00009	0.00796	0.99943	0.00012	0.00902
	5	0.97402	0.00328	0.05519	0.98645	0.00182	0.04133	0.99347	0.00099	0.03051
	6	0.99306	0.00095	0.02853	0.99377	0.00090	0.02804	0.99475	0.00085	0.02736
7 mm	1	0.99085	0.00125	0.03306	0.73033	0.04603	0.20154	0.99364	0.00122	0.03292
	2	0.96462	0.00614	0.06500	0.99161	0.00179	0.03555	0.97903	0.00495	0.05979
	3	0.99871	0.00020	0.01240	0.99854	0.00029	0.01481	0.99922	0.00017	0.01156
	4	0.99921	0.00014	0.00968	0.99854	0.00031	0.01484	0.99872	0.00030	0.01475
	5	0.98458	0.00196	0.04291	0.99058	0.00151	0.03766	0.99161	0.00151	0.03781
	6	0.99465	0.00073	0.02527	0.99074	0.00158	0.03735	0.99217	0.00150	0.03653

M: model number; 1: Aghbaslo model; 2: Alibas model; 3: Balbay and Sahin model; 4: improved Midilli–Kucuk model; 5: Newton model; 6: Page model.

Additionally, Table 6 provides the drying-curve equations and pictures of the final product of the most suitable models for describing the drying process of *Citrus medica* fruits that are dried at various product thicknesses and cabin pressures.

Table 6. The best model and photos obtained during *Citrus medica* freeze-drying experiments.

Thickness (mm)	Cabin Pressure (mbar)	Best Model/Model Equation	Photo
3	0.008	Alibas Model $MR = 0.803695\exp\left(-0.033442t^{0.679641}\right) - 0.000147t + 0.196569$	
	0.010	Alibas Model $MR = 1.260233\exp\left(-0.036462t^{0.506176}\right) - 0.000019 - 0.259875$	
	0.012	Improved Midilli–Kucuk Model $MR = 1.999460\exp\left(0.023095t^{0.457719}\right) - \exp\left(-0.036845t^{0.457719}\right) - 0.122788t^{0.457719}$	
5	0.008	Improved Midilli–Kucuk Model $MR = 2.000004\exp\left(-0.073190t^{0.155535}\right) - \exp\left(-1.205606t^{0.155535}\right) - 0.502613t^{0.155535}$	
	0.010	Balbay and Sahin Model $MR = (1 + 0.364890)\exp\left(-0.017722t^{0.579008}\right) - 0.364830$	
	0.012	Improved Midilli–Kucuk Model $MR = 2.000009\exp\left(0.099977t^{0.242429}\right) - \exp\left(-0.770938t^{0.242429}\right) - 0.599361t^{0.242429}$	
7	0.008	Improved Midilli–Kucuk Model $MR = 2.000778\exp\left(3.17137t^{0.006352}\right) - \exp\left(3.84705t^{0.006352}\right) + 0.795827t^{0.006352}$	
	0.010	Balbay and Sahin Model $MR = (1.516645)\exp\left(-0.007073t^{0.671396}\right) - 0.519823$	
	0.012	Balbay and Sahin Model $MR = (1.685009)\exp\left(-0.004238t^{0.708128}\right) - 0.686328$	

3.3. Results of the Artificial Neural Network

The trained ANN demonstrates promising performance in predicting drying parameters, with low mean squared error (MSE), root mean squared error (RMSE), and high R-squared values on both training and validation datasets. The model effectively captures complex relationships among input features and drying parameters, demonstrating robustness and predictive accuracy across diverse drying conditions and product types. Sensitivity analysis reveals the relative importance of input variables in influencing predicted drying parameters, offering valuable insights for process optimization and control.

In this study, the ANN was used to model the data collected during experiments conducted under various product thicknesses and cabin pressures. In this section, the regression analysis results of the model that was developed based on three inputs (drying time, cabin pressure, and product thickness) and three outputs (MC, MR, and DR) are presented graphically. To ensure the best possible results from the experiment data, the data were clustered into 15% testing, 15% validation, and 70% training. All parameters in the ANN coding were calculated based on these values, and the resulting modeling outcomes are presented in Figure 5. The analysis of all data showed that values above 0.999 were obtained, and in terms of test results, a value above 0.998 was achieved. The ANN model closely approximates a value of 1.0, indicating its validity in modeling the freeze-drying process of *Citrus medica* fruit at various product thicknesses and cabin pressures.
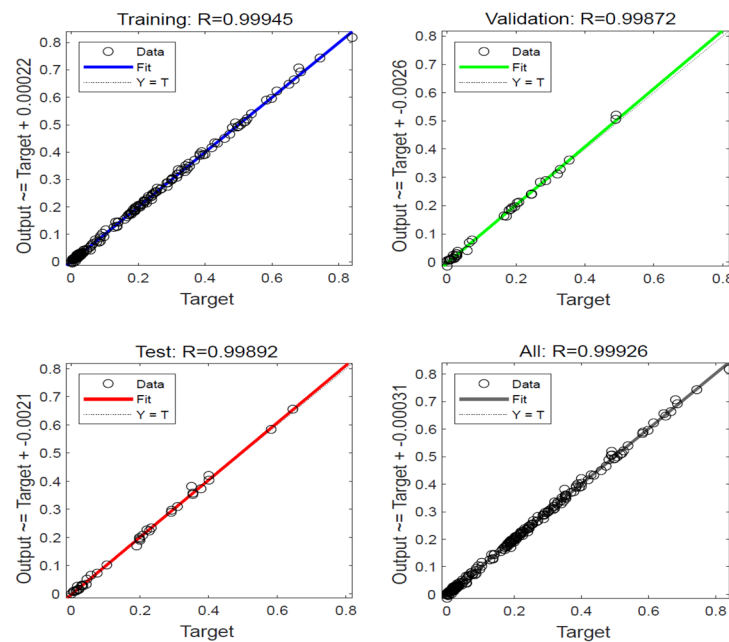

Figure 5. Regression model of predicted and experimental data for freeze-dried *Citrus medica* fruit.

The study compared the predicted and actual MC, MR, and DR data obtained during the freeze-drying of *Citrus medica* fruit at various cabin pressures and thicknesses. The relationship between the experimental values and the predicted values obtained from prediction using ANN models is shown in Figures 6–8. The ANN predicted the MC, MR, and DR of freeze-dried *Citrus medica* fruit at various product thicknesses and cabin pressures with reasonable accuracy, as shown by the plot of experimental and predicted data.
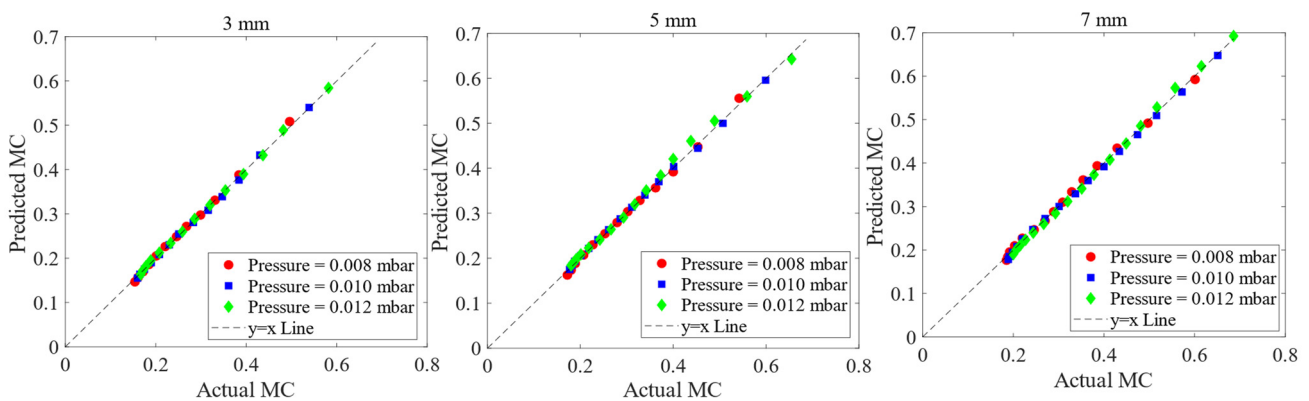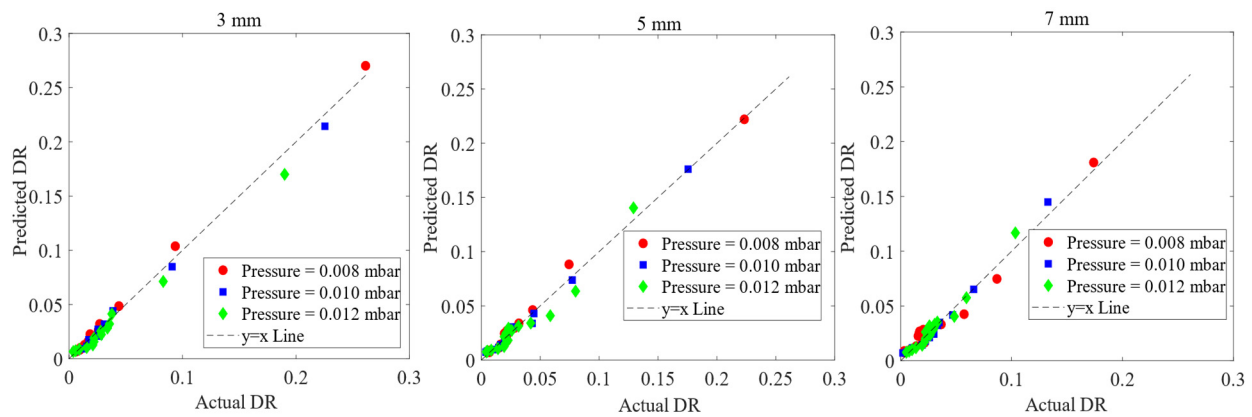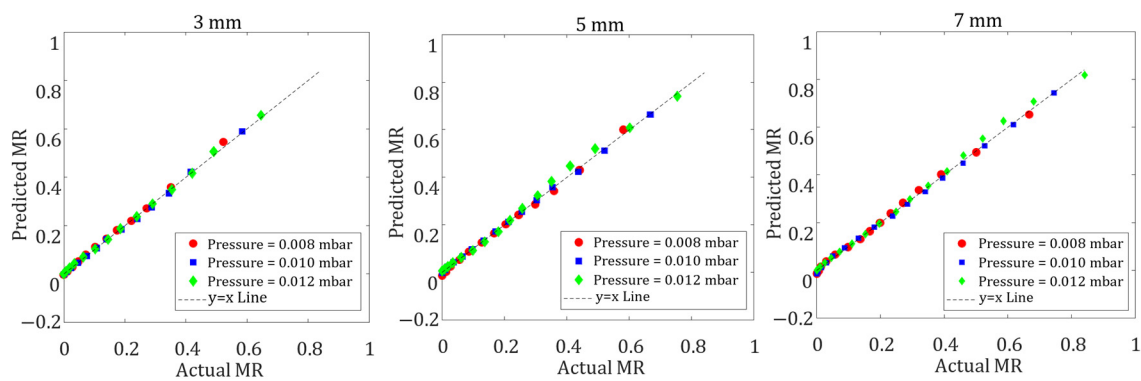

Figure 6. Comparison of experimental MC and predicted MC from ANN modeling.

Figure 7. Comparison of experimental DR and predicted DR from ANN modeling.

Figure 8. Comparison of experimental MR and predicted MR from ANN modeling.

As a result of comparing the experimental MC with the predicted MC from the ANN modeling created by considering various product thicknesses and cabin pressures in Figure 6, the R^2 value was found to be 0.998 and the RMSE value was 0.0064.

As a result of comparing the experimental DR with the predicted DR from the ANN modeling created by considering various product thicknesses and cabin pressures in Figure 7, the R^2 value was found to be 0.984 and the RMSE value was 0.0057.

As a result of comparing the experimental MR with the predicted MR from the ANN modeling created by considering various product thicknesses and cabin pressures in Figure 8, the R^2 value was found to be 0.998 and the RMSE value was 0.010574. It is noteworthy that the thin-layer mathematical models (R^2 = from 0.730 to 0.999; RMSE = from 0.2 to 0.005) demonstrated a strong ability to compete with the extraordinary predictive capabilities of the ANN. This may be attributed to the fact that the drying data used in the study were less complex. However, it is important to consider that the addition of more drying variables could potentially cause semi-empirical models to become erratic, making the use of an ANN more effective in such cases. Although mathematical models can compete with ANNs, an ANN can be used not only to predict MR but also to predict other outputs such as moisture content and drying rate. Therefore, although mathematical models are insufficient to explain the drying process because they only estimate the dimensionless mass loss ratio, the ANN stands out as a superior prediction tool. According to the main findings of this study, the ANN produced outputs that were consistent with the results reported in the literature for various products dried using freeze-drying and other drying techniques [21,62–64]. Utilizing the ANN approach for drying significantly enhanced the overall drying performance. Optimization of input factors and effective management of the drying process can reduce drying time, increase energy efficiency, and enhance profitability.

3.4. Examination of Quality Characteristics of Dried Citrus medica Fruit

Color change, water activity, and effective moisture diffusivity of *Citrus medica* fruits were investigated after drying at various thicknesses and cabin pressures and compared to the fresh fruit. The change in the quality characteristics of the *Citrus medica* fruit after the freeze-drying process is presented in Table 7. Upon examining the experimental data, it was observed that the *Citrus medica* fruit that was 7 mm thick and dried under 0.008 mbar pressure underwent the most significant color change. Additionally, the lightness and yellowness/blueness of the dried product increased as the cabin pressure decreased. It was observed that drying *Citrus medica* fruits under 0.008 mbar pressure resulted in higher lightness and yellowness/blueness values. The lightness decreases as the drying cabin pressure and product thickness increases. Considering the redness/greenness values, it was observed that this value increases as the cabin pressure and product thickness increase. The alterations observed in the L*, a*, and b* values of the freeze-dried end-product were in accordance with the findings of Udomkun et al. (2018) [65]. The water activity of freeze-dried *Citrus medica* fruits varied between 0.4086 ± 0.0104 and 0.5925 ± 0.0064. It was observed that the lowest water activity was measured at a cabin pressure of 0.008 mbar and product thickness of 3 mm. As the thickness of the product and its cabin pressure increase, the water activity of the product also increases. High water activity may cause microorganisms to grow in the product. As a result of freeze-drying experiments carried out with low product thickness and cabin pressure, products with longer storage times can be obtained. As a result of the freeze-drying experiments, the effective moisture diffusivity of the *Citrus medica* fruits was found to be between 4.19×10^{-11} and 21.4×10^{-11} m^2/s. As the cabin pressure decreases and product thickness increases, the effective moisture diffusivity increases. This situation can be explained by the fact that under drying conditions, cabin pressure decreases, which causes moisture in the product to evaporate more easily, thus increasing the drying rate. The effective moisture diffusivity values obtained in this study are within the commonly observed range of 10^{-6} to 10^{-12} m^2/s for the drying of food materials. Specifically, the effective moisture diffusivity values align with those reported in prior studies on linden ($4.13–5.89 \times 10^{-12}$ m^2/s), turmeric ($1.01–9.12 \times 10^{-9}$ m^2/s), and pineapple (24.3×10^{-7} m^2/s) [21,66,67].

Table 7. Quality characteristics of dried *Citrus medica* fruit.

p	Th.	L*	a*	b*	ΔE	h	a_w	$D_{eff} \times 10^{-11}$
	Fresh	14.7 ± 2.1	-3.1 ± 1.4	7.2 ± 3.0	-	-	0.9845 ± 0.0062	-
0.008	3	28.5 ± 1.6	0.4 ± 0.3	9.2 ± 2.2	14.4 ± 0.9	87.5 ± 1.1	0.4086 ± 0.0104	4.38
	5	27.2 ± 2.1	2.5 ± 1.1	19.6 ± 1.9	18.5 ± 0.9	82.7 ± 2.3	0.4979 ± 0.0402	10.8
	7	26.4 ± 1.3	3.1 ± 0.7	23.5 ± 2.6	21.0 ± 0.6	82.4 ± 0.7	0.5622 ± 0.0213	21.4
0.010	3	23.2 ± 1.2	1.1 ± 0.6	8.8 ± 1.7	9.6 ± 1.3	82.9 ± 2.1	0.4479 ± 0.0315	4.20
	5	22.7 ± 1.8	3.0 ± 1.2	17.9 ± 2.2	14.7 ± 0.9	80.5 ± 1.6	0.5152 ± 0.0268	10.2
	7	20.4 ± 1.5	3.4 ± 0.6	22.0 ± 2.5	17.1 ± 0.8	81.2 ± 0.5	0.5771 ± 0.0461	21.3
0.012	3	19.7 ± 2.6	1.7 ± 0.4	7.9 ± 2.0	6.9 ± 0.2	77.9 ± 0.1	0.4891 ± 0.0279	4.19
	5	18.6 ± 2.3	3.4 ± 0.9	16.6 ± 1.3	12.1 ± 1.5	78.4 ± 1.9	0.5213 ± 0.0201	9.7
	7	16.8 ± 1.3	3.6 ± 1.7	21.7 ± 1.9	16.1 ± 0.9	80.6 ± 2.7	0.5925 ± 0.0064	16.8

This study was conducted under specific cabin pressure ranges (from 0.008 to 0.012 mbar), using three different product thicknesses (3, 5, and 7 mm), and controlled laboratory conditions. Experiments were conducted exclusively on *Citrus medica* fruit, with no investigation into the response of different fruit types or varying cabin pressures to the freeze-drying process. While consistent with existing studies in the literature, determining the applicability of the study's findings to other fruit types or drying techniques necessitates testing with different products.

4. Conclusions

In this study, the process of freeze-drying *Citrus medica* fruit was examined under various cabin pressures and thicknesses. Six different mathematical models were applied to the experimental data to determine the thin-layer drying kinetics of the fruit. The experiments were carried out until the product reached equilibrium moisture. The results showed that the quickest drying process occurred when the product was 3 mm thick and dried under 0.008 mbar cabin pressure. Conversely, the longest drying process occurred when the product was 7 mm thick and dried under 0.012 mbar cabin pressure. The experiments concluded that as the product thickness and cabin pressure increase, the drying time also increases. Furthermore, the minimum moisture content was achieved at minimum product thickness and low cabin pressure. The moisture content of the final product was highest when the 7 mm thick product was dried under 0.012 mbar cabin pressure. The freeze-drying experiments of *Citrus medica* fruit conducted at various thicknesses and cabin pressures concluded that the moisture content ranged between 15.4% and 20%. The best mathematical models to fit the experimental data were found to be the Alibas, improved Midilli–Kucuk, and Balbay and Sahin models. An ANN was created using the MC, MR, and DR values obtained during the experiments, and the drying process was well defined based on the R^2 and RMSE obtained. By comparing the experimental MC with the predicted MC from the ANN modeling, which was developed by considering various product thicknesses and cabin pressures, it was concluded that the R^2 value was 0.998 and the RMSE value was 0.0064. Similarly, the comparison of the experimental DR with the predicted DR from the same ANN model indicated that the R^2 value was 0.984 and the RMSE value was 0.0057. Additionally, the comparison of the experimental MR with the predicted MR showed that the R^2 value was 0.998 and the RMSE value was 0.010574. The examination of the color change in dried *Citrus medica* fruit, as a result of freeze-drying experiments, revealed that the lightness (16.8 ± 1.3–28.5 ± 1.6) and yellowness/blueness (7.9 ± 2.0–23.5 ± 2.6) of the final product decreased with increasing cabin pressure (from 0.008 to 0.012 mbar). Results show that as the thickness of freeze-dried *Citrus medica* fruit increased and the drying cabin pressure decreased, the effective moisture diffusivity (4.19×10^{-11}–21.4×10^{-11}) increased. By accurately modeling the drying process and predicting crucial parameters such as MC, MR, and DR, ANNs can contribute to optimizing process conditions, enhancing product quality, and reducing energy consumption. Future research may explore the integration of ANNs with advanced optimization techniques and experimental validation to further enhance model accuracy and applicability in real-world food processing scenarios.

Author Contributions: Conceptualization, M.E.T., B.Ş. and S.V.; methodology, M.E.T., B.Ş. and S.V.; software, M.E.T. and S.V.; validation, M.E.T. and B.Ş.; formal analysis, M.E.T., B.Ş. and S.V.; investigation, M.E.T., B.Ş. and S.V.; data curation, M.E.T. and S.V.; writing—original draft preparation, M.E.T. and S.V.; writing—review and editing, M.E.T. and B.Ş.; visualization, M.E.T.; B.Ş. and S.V.; supervision, B.Ş. All authors have read and agreed to the published version of the manuscript.

Data Availability Statement: The original contributions presented in the study are included in the article; further inquiries can be directed to the corresponding author.

Conflicts of Interest: The authors declare no conflicts of interest.

References

1. Ladaniya, M. Commercial Fresh Citrus Cultivars and Producing Countries. In *Citrus Fruit*; Academic Press: Cambridge, MA, USA, 2023; pp. 23–91, ISBN 978-0-323-99306-7.
2. Chhikara, N.; Kour, R.; Jaglan, S.; Gupta, P.; Gat, Y.; Panghal, A. Citrus Medica: Nutritional, Phytochemical Composition and Health Benefits—A Review. *Food Funct.* **2018**, *9*, 1978–1992. [CrossRef] [PubMed]
3. Panara, K.; Joshi, K.; Nishteswar, K. A Review on Phytochemical and Pharmacological Properties of Citrus Medica Linn. *Int. J. Pharm. Biol. Arch.* **2012**, *3*, 1292–1297.

4. Ballistreri, G.; Fabroni, S.; Romeo, F.V.; Timpanaro, N.; Amenta, M.; Rapisarda, P. *Anthocyanins and Other Polyphenols in Citrus Genus: Biosynthesis, Chemical Profile, and Biological Activity*, 2nd ed.; Elsevier: Amsterdam, The Netherlands, 2019; ISBN 9780128137680.

5. Addo, P.W.; Chauvin-Bossé, T.; Taylor, N.; MacPherson, S.; Paris, M.; Lefsrud, M. Freeze-Drying Cannabis Sativa L. Using Real-Time Relative Humidity Monitoring and Mathematical Modeling for the Cannabis Industry. *Ind. Crop. Prod.* **2023**, *199*, 116754. [CrossRef]

6. Thamkaew, G.; Sjöholm, I.; Galindo, F.G. A Review of Drying Methods for Improving the Quality of Dried Herbs. *Crit. Rev. Food Sci. Nutr.* **2021**, *61*, 1763–1786. [CrossRef] [PubMed]

7. Salehi, F. Recent Progress and Application of Freeze Dryers for Agricultural Product Drying. *ChemBioEng Rev.* **2023**, *10*, 618–627. [CrossRef]

8. Ma, Y.; Yi, J.; Jin, X.; Li, X.; Feng, S.; Bi, J. Freeze-Drying of Fruits and Vegetables in Food Industry: Effects on Phytochemicals and Bioactive Properties Attributes—A Comprehensive Review. *Food Rev. Int.* **2023**, *39*, 6611–6629. [CrossRef]

9. Biernacka, B.; Dziki, D.; Rudy, S.; Krzykowski, A.; Polak, R.; Dziki, L. Influence of Pretreatments and Freeze-Drying Conditions of Strawberries on Drying Kinetics and Physicochemical Properties. *Processes* **2022**, *10*, 1588. [CrossRef]

10. Zhao, C.C.; Ameer, K.; Eun, J.B. Effects of Various Drying Conditions and Methods on Drying Kinetics and Retention of Bioactive Compounds in Sliced Persimmon. *LWT* **2021**, *143*, 111149. [CrossRef]

11. Lopez-Quiroga, E.; Prosapio, V.; Fryer, P.J.; Norton, I.T.; Bakalis, S. Model Discrimination for Drying and Rehydration Kinetics of Freeze-Dried Tomatoes. *J. Food Process. Eng.* **2020**, *43*, e13192. [CrossRef]

12. Taskin, O. Evaluation of Freeze Drying for Whole, Half Cut and Puree Black Chokeberry (*Aronia melanocarpa* L.). *Heat Mass Transf.* **2020**, *56*, 2503–2513. [CrossRef]

13. Baeghbali, V.; Ngadi, M.; Niakousari, M. Effects of Ultrasound and Infrared Assisted Conductive Hydro-Drying, Freeze-Drying and Oven Drying on Physicochemical Properties of Okra Slices. *Innov. Food Sci. Emerg. Technol.* **2020**, *63*, 102313. [CrossRef]

14. Pinar, H.; Çetin, N.; Ciftci, B.; Karaman, K.; Kaplan, M. Biochemical Composition, Drying Kinetics and Chromatic Parameters of Red Pepper as Affected by Cultivars and Drying Methods. *J. Food Compos. Anal.* **2021**, *102*, 103976. [CrossRef]

15. Winiczenko, R.; Kaleta, A.; Górnicki, K. Application of a Moga Algorithm and Ann in the Optimization of Apple Drying and Rehydration Processes. *Processes* **2021**, *9*, 1415. [CrossRef]

16. Azadbakht, M.; Aghili, H.; Ziaratban, A.; Torshizi, M.V. Application of Artificial Neural Network Method to Exergy and Energy Analyses of Fluidized Bed Dryer for Potato Cubes. *Energy* **2017**, *120*, 947–958. [CrossRef]

17. Omari, A.; Behroozi-Khazaei, N.; Sharifian, F. Drying Kinetic and Artificial Neural Network Modeling of Mushroom Drying Process in Microwave-Hot Air Dryer. *J. Food Process. Eng.* **2018**, *41*, 1–10. [CrossRef]

18. Sarimeseli, A.; Coskun, M.A.; Yuceer, M. Modeling Microwave Drying Kinetics of Thyme (Thymus vulgaris L.) Leaves Using ANN Methodology and Dried Product Quality. *J. Food Process. Preserv.* **2014**, *38*, 558–564. [CrossRef]

19. Karakaplan, N.; Goz, E.; Tosun, E.; Yuceer, M. Kinetic and Artificial Neural Network Modeling Techniques to Predict the Drying Kinetics of *Mentha spicata* L. *J. Food Process. Preserv.* **2019**, *43*, e14142. [CrossRef]

20. Jahedi Rad, S.; Kaveh, M.; Sharabiani, V.R.; Taghinezhad, E. Fuzzy Logic, Artificial Neural Network and Mathematical Model for Prediction of White Mulberry Drying Kinetics. *Heat Mass Transf.* **2018**, *54*, 3361–3374. [CrossRef]

21. Selvi, K.Ç.; Alkhaled, A.Y.; Yıldız, T. Application of Artificial Neural Network for Predicting the Drying Kinetics and Chemical Attributes of Linden (*Tilia platyphyllos* Scop.) during the Infrared Drying Process. *Processes* **2022**, *10*, 2069. [CrossRef]

22. Zalpouri, R.; Singh, M.; Kaur, P.; Kaur, A.; Gaikwad, K.K.; Singh, A. Drying Kinetics, Physicochemical and Thermal Analysis of Onion Puree Dried Using a Refractance Window Dryer. *Processes* **2023**, *11*, 700. [CrossRef]

23. Khaled, A.Y.; Kabutey, A.; Selvi, K.Ç.; Mizera, Č.; Hrabe, P.; Herák, D. Application of Computational Intelligence in Describing the Drying Kinetics of Persimmon Fruit (*Diospyros kaki*) during Vacuum and Hot Air Drying Process. *Processes* **2020**, *8*, 544. [CrossRef]

24. Midilli, A.; Kucuk, H. Development of a New Curve Equation Representing Thin Layer Drying Process. *Energy Sources Part A Recovery Util. Environ. Eff.* **2023**, *45*, 9717–9730. [CrossRef]

25. Alibaş, I. Microwave Drying of Grapevine (*Vitis vinifera* L.) Leaves and Determination of Some Quality Parameters. *J. Agric. Sci. Bilim. Derg.* **2012**, *18*, 43–53. [CrossRef]

26. Balbay, A.; Şahin, Ö. Microwave Drying Kinetics of a Thin-Layer Liquorice Root. *Dry. Technol.* **2012**, *30*, 859–864. [CrossRef]

27. Omolola, A.O.; Jideani, A.I.O.; Kapila, P.F. Modeling Microwave Drying Kinetics and Moisture Diffusivity of Mabonde Banana Variety. *Int. J. Agric. Biol. Eng.* **2014**, *7*, 107–113. [CrossRef]

28. Ganesapillai, M.; Regupathi, I.; Murugesan, T. Modeling of Thin Layer Drying of Banana (*Nendran* Spp.) under Microwave, Convective and Combined Microwave-Convective Processes. *Chem. Prod. Process Model.* **2011**, *6*, 1–29. [CrossRef]

29. Kucuk, H.; Midilli, A.; Kilic, A.; Dincer, I. A Review on Thin-Layer Drying-Curve Equations. *Dry. Technol.* **2014**, *32*, 757–773. [CrossRef]

30. Dash, K.; Bhagya Raj, G.; Gayary, M. Application of Neural Networks in Optimizing Different Food Processes Case Study. In *Mathematical and Statistical Applications in Food Engineering*; CRC Press: Boca Raton, FL, USA, 2020; pp. 346–362.

31. Raj, G.V.S.B.; Dash, K.K. Microencapsulation of Dragon Fruit Peel Extract by Freeze-Drying Using Hydrocolloids: Optimization by Hybrid Artificial Neural Network and Genetic Algorithm. *Food Bioprocess Technol.* **2022**, *15*, 2035–2049. [CrossRef]

32. Li, Z.; Wang, Y.; Shi, Q.; Gao, J.; Zhang, C.; Fan, X.; Liu, Y. Drying Characteristics and Neural Network Models of Contact Ultrasound Strengthened Cold Air Drying on Yam. *Heat Mass Transf.* **2023**, *59*, 1109–1120. [CrossRef]

33. Thapliyal, D.; Shrivastava, R.; Verros, G.D.; Verma, S.; Arya, R.K.; Sen, P.; Prajapati, S.C.; Chahat; Gupta, A. Modeling of Triphenyl Phosphate Surfactant Enhanced Drying of Polystyrene/p-Xylene Coatings Using Artificial Neural Network. *Processes* **2024**, *12*, 260. [CrossRef]

34. Barriga, R.; Romero, M.; Nettleton, D.; Hassan, H. Advanced Data Modeling for Industrial Drying Machine Energy Optimization. *J. Supercomput.* **2022**, *78*, 16820–16840. [CrossRef]

35. Çetin, N. Prediction of Moisture Ratio and Drying Rate of Orange Slices Using Machine Learning Approaches. *J. Food Process. Preserv.* **2022**, *46*, e17011. [CrossRef]

36. Dalvi-Isfahan, M. A Comparative Study on the Efficiency of Two Modeling Approaches for Predicting Moisture Content of Apple Slice during Drying. *J. Food Process. Eng.* **2020**, *43*, e13527. [CrossRef]

37. Chasiotis, V.K.; Tzempelikos, D.A.; Filios, A.E.; Moustris, K.P. Artificial Neural Network Modelling of Moisture Content Evolution for Convective Drying of Cylindrical Quince Slices. *Comput. Electron. Agric.* **2020**, *172*, 105074. [CrossRef]

38. Paturi, U.M.R.; Cheruku, S.; Reddy, N.S. The Role of Artificial Neural Networks in Prediction of Mechanical and Tribological Properties of Composites—A Comprehensive Review. *Arch. Comput. Methods Eng.* **2022**, *29*, 3109–3149. [CrossRef]

39. Albelwi, S.; Mahmood, A. A Framework for Designing the Architectures of Deep Convolutional Neural Networks. *Entropy* **2017**, *19*, 242. [CrossRef]

40. Šovljanski, O.; Lončar, B.; Pezo, L.; Saveljić, A.; Tomić, A.; Brunet, S.; Filipović, V.; Filipović, J.; Čanadanović-Brunet, J.; Ćetković, G.; et al. Unlocking the Potential of the ANN Optimization in Sweet Potato Varieties Drying Processes. *Foods* **2023**, *13*, 134. [CrossRef]

41. Kayri, M. Predictive Abilities of Bayesian Regularization and Levenberg-Marquardt Algorithms in Artificial Neural Networks: A Comparative Empirical Study on Social Data. *Math. Comput. Appl.* **2016**, *21*, 20. [CrossRef]

42. Rehman, K.U.; Shatanawi, W.; Mustafa, Z. Levenberg-Marquardt Backpropagation Neural Networking (LMB-NN) Analysis of Hydrodynamic Forces in Fluid Flow over Multiple Cylinders. *AIP Adv.* **2024**, *14*, 025051. [CrossRef]

43. Touil, A.; Chemkhi, S.; Zagrouba, F. Moisture Diffusivity and Shrinkage of Fruit and Cladode of Opuntia Ficus-Indica during Infrared Drying. *J. Food Process.* **2014**, *2014*, 1–9. [CrossRef]

44. Chen, D.; Zheng, Y.; Zhu, X. Determination of Effective Moisture Diffusivity and Drying Kinetics for Poplar Sawdust by Thermogravimetric Analysis under Isothermal Condition. *Bioresour. Technol.* **2012**, *107*, 451–455. [CrossRef] [PubMed]

45. Zeng, Z.; Han, C.; Wang, Q.; Yuan, H.; Zhang, X.; Li, B. Analysis of Drying Characteristic, Effective Moisture Diffusivity and Energy, Exergy and Environment Performance Indicators during Thin Layer Drying of Tea in a Convective-Hot Air Dryer. *Front. Sustain. Food Syst.* **2024**, *8*, 1371696. [CrossRef]

46. Taner, T. Optimisation Processes of Energy Efficiency for a Drying Plant: A Case of Study for Turkey. *Appl. Therm. Eng.* **2015**, *80*, 247–260. [CrossRef]

47. Kovaci, T.; Dikmen, E.; Şahin, A.S. Drying Behaviors of Mint Leaves in Vacuum Freeze Drying. *El-Cezeri J. Sci. Eng.* **2020**, *7*, 371–384. [CrossRef]

48. Kovacı, T.; Dikmen, E.; Şahin, A.Ş. Energy and Exergy Analysis of Freeze-Drying of Mint Leaves. *J. Food Process. Eng.* **2020**, *43*, e13528. [CrossRef]

49. Chen, B.L.; Jang, J.H.; Amani, M.; Yan, W.M. Numerical and Experimental Study on the Heat and Mass Transfer of Kiwifruit during Vacuum Freeze-Drying Process. *Alex. Eng. J.* **2023**, *73*, 427–442. [CrossRef]

50. El-Mesery, H.S.; Huang, H.; Hu, Z.; Kaveh, M.; Qenawy, M. Experimental Performance Analysis of an Infrared Heating System for Continuous Applications of Drying. *Case Stud. Therm. Eng.* **2024**, *59*, 104522. [CrossRef]

51. Zhang, Y.; Lu, Y.; Huang, D.; Zhao, H.; Huang, S.; Zhang, L.; Gong, G.; Li, L. Infrared Drying Characteristics and Optimization of Ginseng. *Case Stud. Therm. Eng.* **2024**, *57*, 104334. [CrossRef]

52. El-Beltagi, H.S.; Khan, A.; Shah, S.T.; Basit, A.; Sajid, M.; Hanif, M.; Mohamed, H.I. Improvement of Postharvest Quality, Secondary Metabolites, Antioxidant Activity and Quality Attributes of *Prunus persica* L. Subjected to Solar Drying and Slice Thickness. *Saudi J. Biol. Sci.* **2023**, *30*, 103866. [CrossRef]

53. Korese, J.K.; Achaglinkame, M.A. Convective Drying of Gardenia Erubescens Fruits: Effect of Pretreatment, Slice Thickness and Drying Air Temperature on Drying Kinetics and Product Quality. *Heliyon* **2024**, *10*, e25968. [CrossRef]

54. Dhake, K.; Jain, S.K.; Jagtap, S.; Pathare, P.B. Effect of Pretreatment and Temperature on Drying Characteristics and Quality of Green Banana Peel. *AgriEngineering* **2023**, *5*, 2064–2078. [CrossRef]

55. Man, X.; Li, L.; Fan, X.; Zhang, H.; Lan, H.; Tang, Y.; Zhang, Y. Evolution and Modelling of the Moisture Diffusion in Walnuts during the Combination of Hot Air and Microwave–Vacuum Drying. *Agriculture* **2024**, *14*, 190. [CrossRef]

56. Zheng, Y.; Zhang, S.; Yang, L.; Wei, B.; Guo, Q. Prevention of the Quality Degradation of Antarctic Krill (*Euphausia superba*) Meal through Two-Stage Drying. *Foods* **2024**, *13*, 1706. [CrossRef] [PubMed]

57. Stephenus, F.N.; Benjamin, M.A.Z.; Anuar, A.; Awang, M.A. Effect of Temperatures on Drying Kinetics, Extraction Yield, Phenolics, Flavonoids, and Antioxidant Activity of *Phaleria macrocarpa* (Scheff.) Boerl. (Mahkota Dewa) Fruits. *Foods* **2023**, *12*, 2859. [CrossRef] [PubMed]

58. Hii, C.L.; Law, C.L.; Cloke, M.; Suzannah, S. Thin Layer Drying Kinetics of Cocoa and Dried Product Quality. *Biosyst. Eng.* **2009**, *102*, 153–161. [CrossRef]

59. Doymaz, İ. Drying Kinetics, Rehydration and Colour Characteristics of Convective Hot-Air Drying of Carrot Slices. *Heat Mass Transf.* **2017**, *53*, 25–35. [CrossRef]

60. Taheri-Garavand, A.; Meda, V. Drying Kinetics and Modeling of Savory Leaves under Different Drying Conditions. *Int. Food Res. J.* **2018**, *25*, 1357–1364.

61. Dundar, A.N.; Sahin, O.I.; Parlak, M.E.; Saricaoglu, F.T. Drying Kinetics and Change in Bioactive Compounds of Edible Flowers: Prunus Domestica. *J. Food Process. Eng.* **2023**, *46*, e14405. [CrossRef]

62. Menlik, T.; Özdemir, M.B.; Kirmaci, V. Determination of Freeze-Drying Behaviors of Apples by Artificial Neural Network. *Expert Syst. Appl.* **2010**, *37*, 7669–7677. [CrossRef]

63. Tarafdar, A.; Shahi, N.C.; Singh, A. Freeze-Drying Behaviour Prediction of Button Mushrooms Using Artificial Neural Network and Comparison with Semi-Empirical Models. *Neural Comput. Appl.* **2019**, *31*, 7257–7268. [CrossRef]

64. Bai, J.W.; Xiao, H.W.; Ma, H.L.; Zhou, C.S. Artificial Neural Network Modeling of Drying Kinetics and Color Changes of Ginkgo Biloba Seeds during Microwave Drying Process. *J. Food Qual.* **2018**, *2018*, 3278595. [CrossRef]

65. Udomkun, P.; Argyropoulos, D.; Nagle, M.; Mahayothee, B.; Oladeji, A.E.; Müller, J. Changes in Microstructure and Functional Properties of Papaya as Affected by Osmotic Pre-Treatment Combined with Freeze-Drying. *J. Food Meas. Charact.* **2018**, *12*, 1028–1037. [CrossRef]

66. Taşkin, O.; İzlı, N. Effect of Microwave, Infrared and Freeze Drying Methods on Drying Kinetics, Effective Moisture Diffusivity and Color Properties of Turmeric. *J. Agric. Sci. Bilim. Derg.* **2019**, *25*, 334–345. [CrossRef]

67. Sarkar, T.; Salauddin, M.; Hazra, S.K.; Chakraborty, R. Artificial Neural Network Modelling Approach of Drying Kinetics Evolution for Hot Air Oven, Microwave, Microwave Convective and Freeze Dried Pineapple. *SN Appl. Sci.* **2020**, *2*, 1621. [CrossRef]